

Figure S1. OGD/R induces PANoptosis activation in R28 cells. A. Western blotting showed the dynamic changes in apoptosis-related protein levels in R28 cells following OGD/R. **B-D.** Relative band intensity of BAX (B), cleaved-Caspase-3 (C) and cleaved-Caspase-7 (D). **E.** Western blotting showed the dynamic changes in necroptosis-related protein levels in R28 cells following OGD/R. **F-I.** Relative band intensity of RIP1 (F), RIP3 (G), p-RIP3 (H) and p-MLKL (I). **J.** LDH release ratio in R28 cells under different treatments were determined by LDH release assay. **K.** Western blotting showed the dynamic changes in pyroptosis-related protein levels in R28 cells following OGD/R. **L-N.** Relative band intensity of NLRP3 (L), N-GSDMD (M) and N-GSDME (N). Data are presented as the mean \pm SD (n = 3-4). *p < 0.05, **p < 0.01, ****p < 0.001 (compared with the R28^{Norm} group were performed using one-way analysis of variance followed by Tukeys post-hoc test).

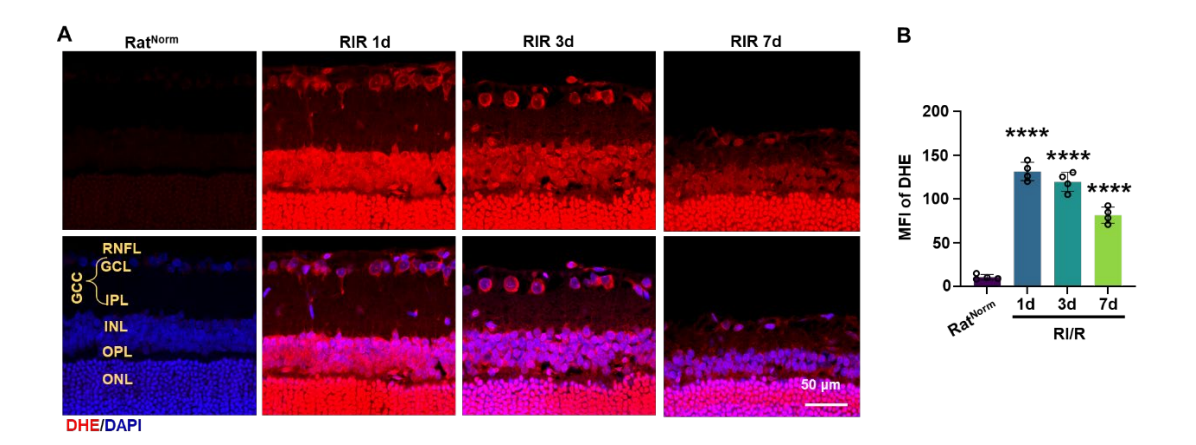


Figure S2. RI/R induces dynamic oxidative stress in rat retinas. A. Representative images of retinal sections stained with dihydroethidium (DHE, red) to detect superoxide production. The cell nucleus was stained by DAPI (blue). B. Quantification of DHE fluorescence intensity. Data are presented as the mean \pm SD (n = 4 rats). ****p < 0.0001 (compared with the Rat^{Norm} group were performed using one-way analysis followed by Tukeys post-hoc test).

PDSD

HO

S

OH

CDI, Dry DMF

DDPD

OH

$$113^{O}$$

OH

 113^{O}
 113^{O}

P1

P1

PDSD

DDPD

DDPD

OH

 113^{O}
 113^{O}

P1

Figure S3. Schematic representation of the synthesis route for P1.

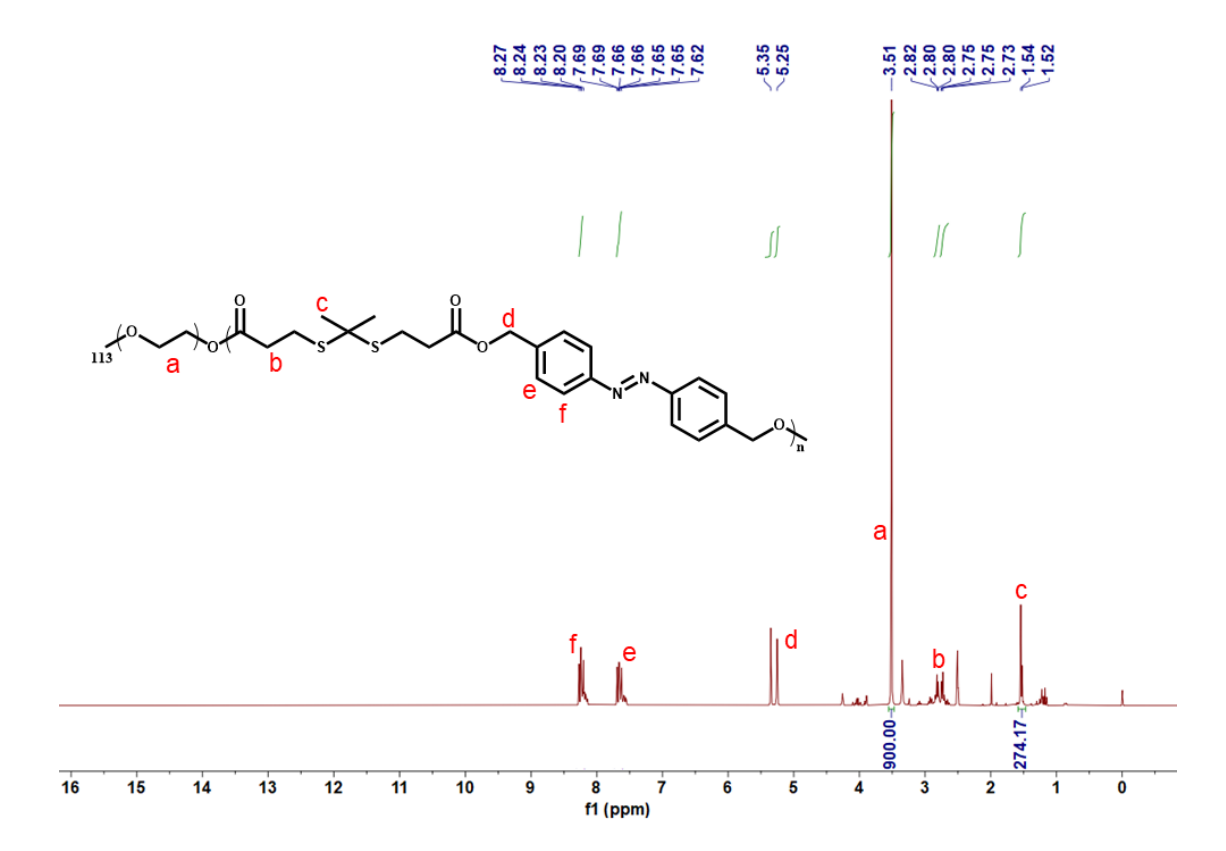


Figure S4. Characterization of P1 in DMSO-d6 by nuclear magnetic resonance (1H-NMR) spectroscopy.

Figure S5. Mechanism of degradation of MT-NPs by accumulated ROS.

Figure S6. Mechanism of degradation of MT-NPs under hypoxia.

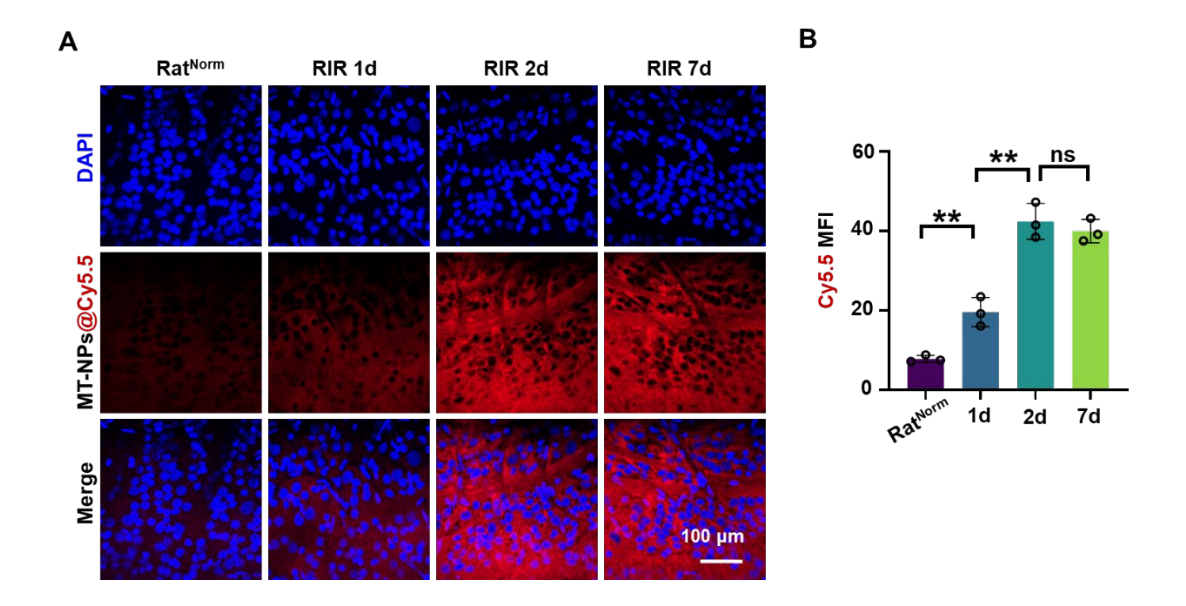


Figure S7. Intracellular uptake of MT-NPs@Cy5.5 by retinal cells. A. Representative images of rat retinal whole-mounts on day 1, 2, 7 after intravitreal injection of MT-NPs@Cy5.5. The red fluorescence came from Cy5.5 (red). The cell nucleus was stained by DAPI (blue). **B.** Quantification of mean fluorescence intensity (MFI) of MT-NPs@Cy5.5 in retinal whole-mounts. Data are presented as the mean \pm SD (n = 3 rats). ns, not significant, **p < 0.01 (comparisons between different groups were performed using one-way analysis of variance followed by Tukeys post-hoc test).

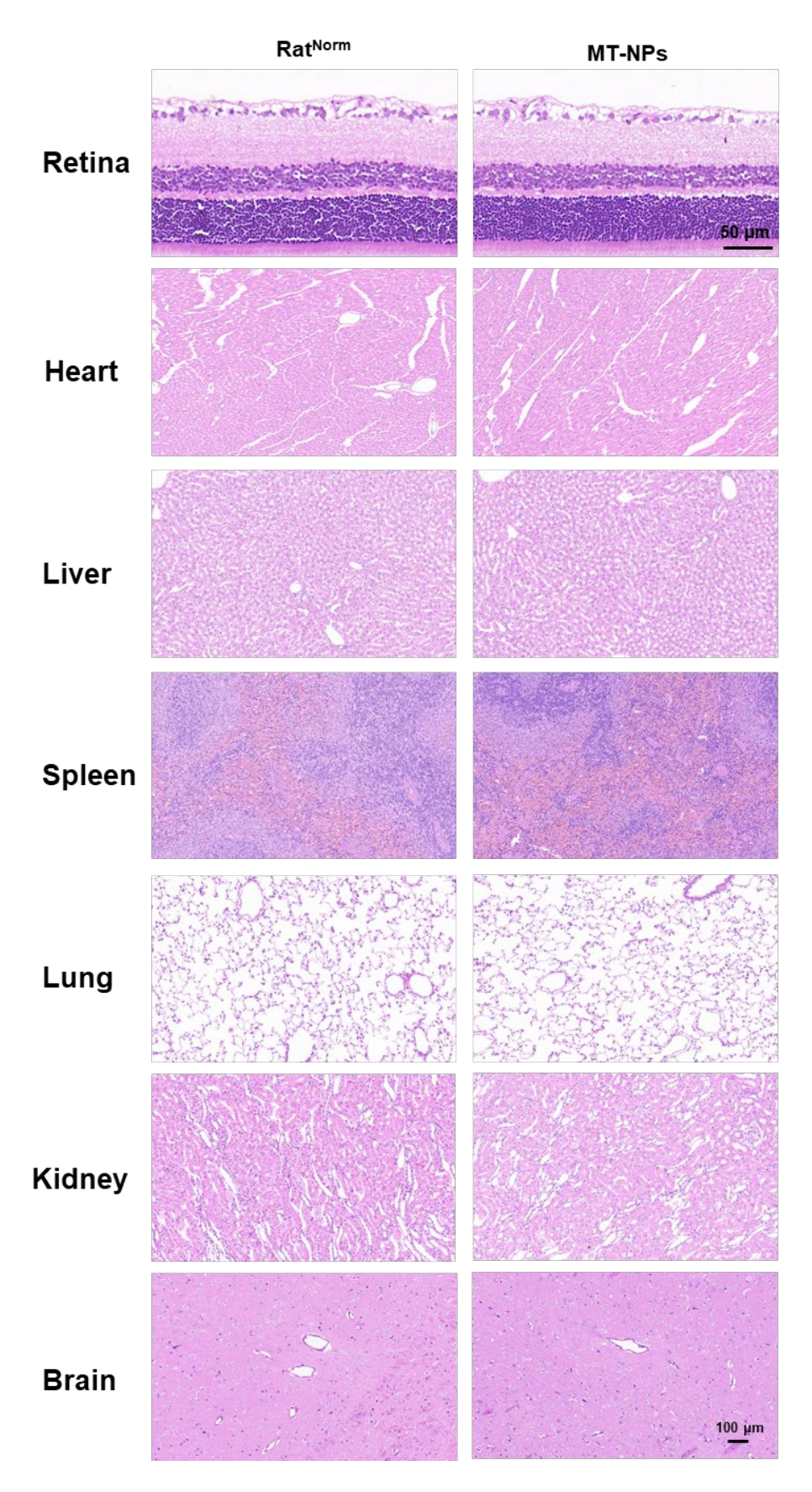


Figure S8. MT-NPs does not cause systemic vital organ damage on day 14 after intravitreal injection in rats (n = 3 rats).

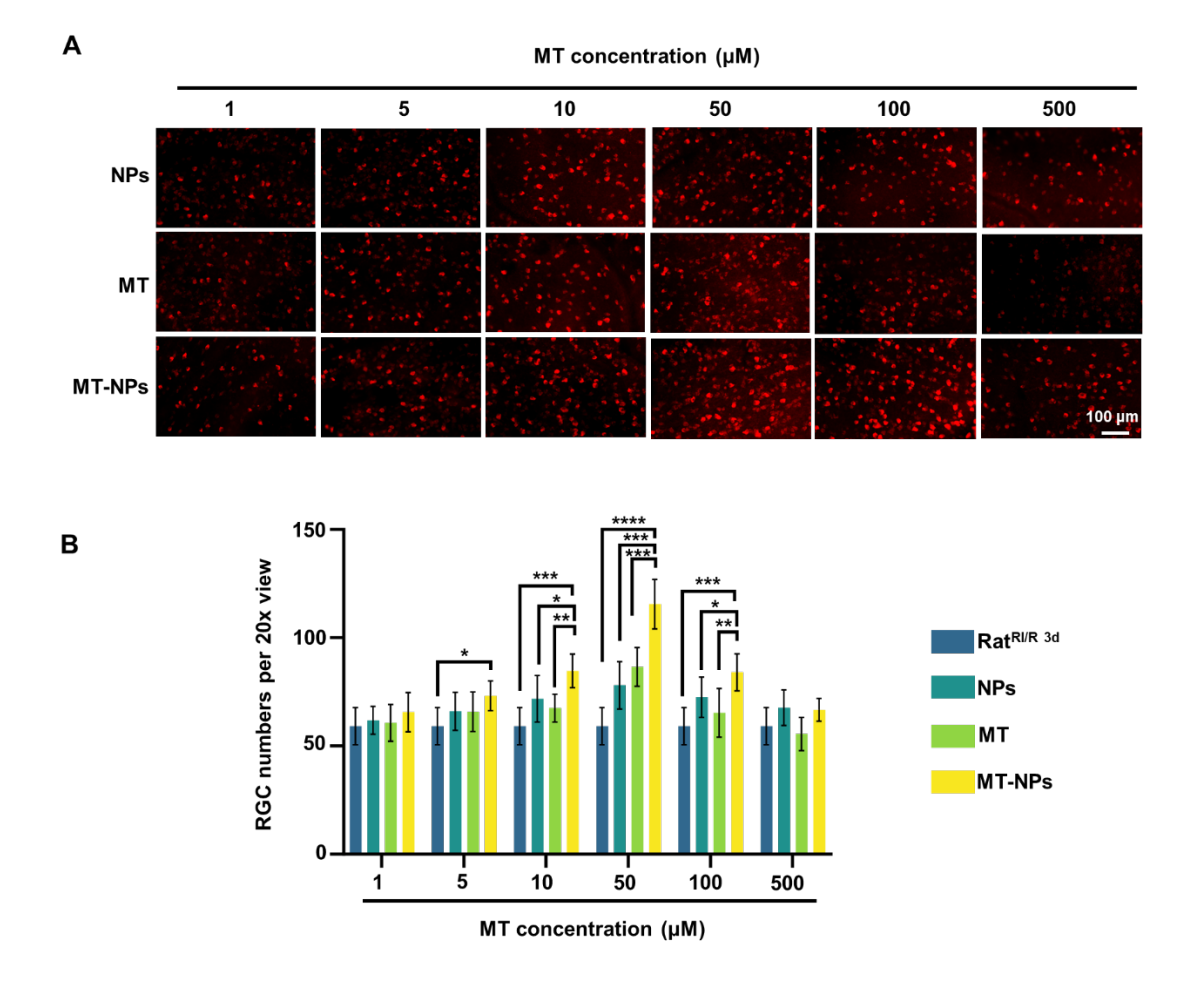


Figure S9. *In vivo* protection of rat^{RI/R} with NPs, MT and MT-NPs at different concentrations. A. RBPMS labeled RGCs in flattening of rat retinas under different treatments. B. Quantification of RGCs per field of view. Data are presented as the mean \pm SD (n = 4-6 rats). *p < 0.05, **p < 0.01, ****p < 0.001, ****p < 0.0001 (comparisons between different groups were performed using Student t-test).

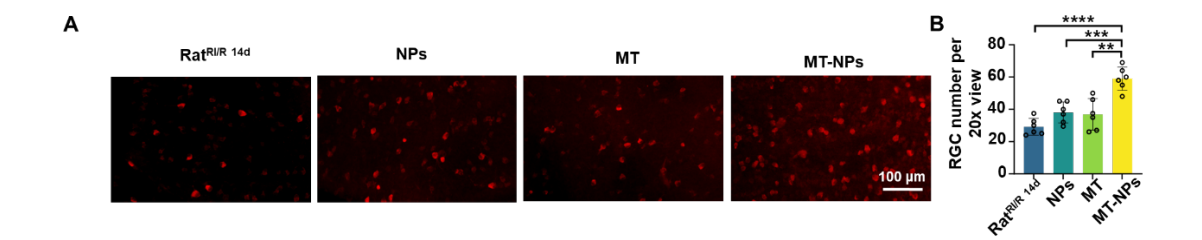


Figure S10. MT-NPs preserve RGCs on day 14 after RI/R injury. A. RBPMS labeled RGCs in flattening of rat retinas under different treatments. **B.** Quantification of RGCs per field of view. Data are presented as the mean \pm SD (n = 6 rats). **p < 0.01, ***p < 0.001, ****p < 0.0001 (comparisons between different groups were performed using Student t-test).

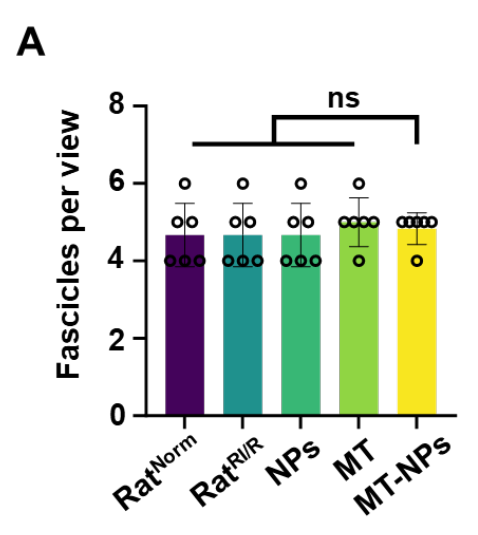


Figure S11. The number of fascicles per view in rat retinas. A. Data are presented as the mean \pm SD (n = 6 rats). ns, not significant (comparisons between different groups were performed using Student t-test).

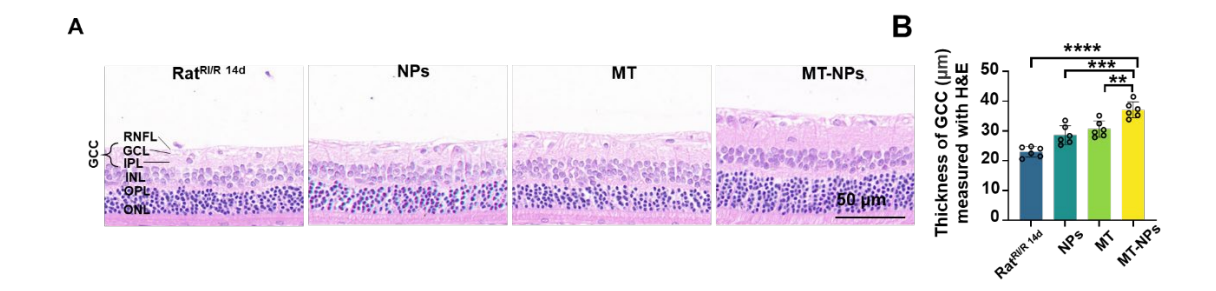


Figure S12. MT-NPs preserve retinal structure on day 14 following RI/R injury. A. H&E staining of rat retinas under different treatments. **B.** The thickness of GCC with different treatments measured via H&E staining (n = 6 rats). **p < 0.01, ***p < 0.001, ***p < 0.0001 (comparisons between different groups were performed using Student t-test).

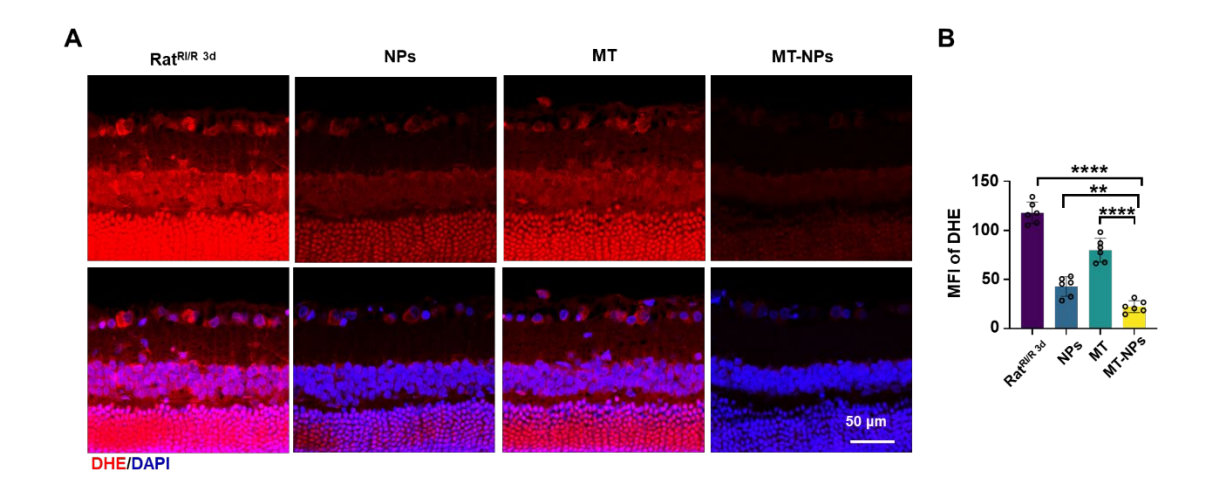


Figure S13. MT-NPs mitigate retinal oxidative stress in vivo. A. DHE staining (red) of retinal sections. Nuclei were stained with DAPI (blue). B. Quantification of DHE fluorescence intensity. Data are presented as the mean \pm SD (n = 6 rats). **p < 0.01, ****p < 0.0001 (comparisons between different groups were performed using Student t-test).

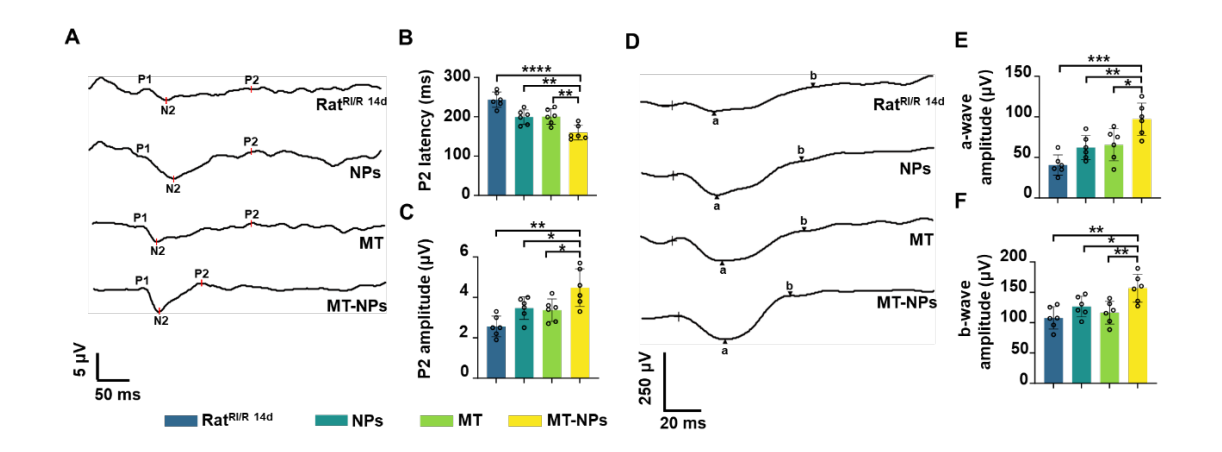


Figure S14. MT-NPs improve visual function on day 14 after RI/R injury. A. The FERG results of rats under various treatments. **B.** Quantification of FVEP P2 latency. C. Quantification of FVEP P2 amplitude. **D.** The FERG results of rats under various treatment. **E.** Quantification of FERG a-wave amplitudes. **F.** Quantification of FERG b-wave amplitudes. Data are presented as the mean \pm SD (n = 6 rats). *p < 0.05, **p < 0.01, ***p < 0.001, ****p < 0.0001 (Comparisons between different groups were performed using Student t-test).

Table S1. Characterization data for P1.

	degree of polymerization	Drug loading content	Encapsulation Efficiency
		(%)	(%)
P1	23	6.47	58